

Lithium Electrochemical Tuning for Electrocatalysis

Zhiyi Lu, Kun Jiang, Guangxu Chen, Haotian Wang,* and Yi Cui*

Electrocatalysis is of great importance to a variety of energy conversion processes, where developing highly efficient catalysts is critical. While common strategies involve screening a wide range of materials with new chemical compositions or structures, a different approach to continuously, controllably, and effectively tune the electronic properties of existing catalytic materials for optimized activities has been demonstrated recently. Inspired by studies in lithium-ion batteries, systematical lithium electrochemical tuning (LiET) methods such as Li intercalation, extraction, cycling, and strain engineering, are employed to effectively tune the electronic structures of different existing catalysts and thus improve their catalytic activities dramatically. Herein, the advantages of the LiET method in electrocatalysis are introduced, and then some recent representative examples in improving the performances of important electrochemical reactions are reviewed briefly. Lastly, a few promising directions on extending the applications of the LiET method in electrocatalysis are proposed.

1. Introduction

Several water-based electrochemical reactions, such as hydrogen evolution reaction (HER),^[1] oxygen evolution reaction (OER),^[2] oxygen reduction reaction (ORR),^[3] hydrogen oxidation reaction,^[4] and carbon dioxide reduction reaction (CO₂RR),^[5] are critical half-cell reactions for developing large-scale clean energy storage and usage and thus mitigating the increasing greenhouse gas emission.^[6] To maximize the energy conversion efficiencies, highly efficient catalysts with reduced overpotentials for these electrochemical reactions are required. In fact, the strong correlation between the electronic structure

and the catalytic activity of the catalyst has been revealed by both theoretical simulations and experimental demonstrations.^[7] The electronic property of a highly active electrocatalyst should satisfy strict requirements: the interactions between the atomic sites and the reactants/products should be not too weak nor too strong, which ensure smooth electron transfers between the catalysts and the reagents, and at the same time facilitates the releasing of the products.^[8] For instance, guided by theoretical simulations, scientists discovered that the edge sites of 2D materials, such as the transition metal dichalcogenides (TMDs) (MoS₂/Se₂ and WS₂/Se₂), possess a electronic structure which binds the atomic hydrogen properly, and can thus catalyze HER at a relatively low overpotential comparable to the state-of-art Pt-based catalyst in acid media.^[6a,9]

While continuously searching materials with new chemical compositions and morphologies has been proved to be an interesting direction to pursue, another effective approach, that is employing lithium to electrochemically tune the electronic structure of existing materials in organic electrolytes for optimal catalytic activities, has been demonstrated by our group.^[10] This lithium electrochemical tuning (LiET) strategy can offer a wide potential window (up to several volts) to continuously, precisely and directionally control the electronic structure of active sites, resulting in much tuned activities of existing catalysts to serve the purposes. In the past several decades, electrochemical reactions of diverse materials with lithium ions in organic electrolytes have been well investigated and understood accompanied with the rapid development of lithium-ion batteries (LIBs) technology.^[11] Based on the different reaction mechanisms in LIBs as well as materials, the catalyst tuning (**Scheme 1**) processes can be summarized and differentiated as follows: a) electrochemical intercalation/de-intercalation of lithium ions into the interlayer of materials,^[12] such as layered transition metal dichalcogenides (e.g., MoS₂) and lithium transition metal oxides (e.g., LiCoO₂^[13]), can tune the oxidation state, electronic structure and local coordination configuration of the catalytic site; b) lithium induced conversion reactions^[14] on various metal/metal oxides (e.g., Co₃O₄ and NiO) give rise to much higher surface areas and more abundant grain boundaries/defects; c) electrochemical lithium alloying and dealloying on various metal nanoparticles (e.g., Sn, Pb, Au, Pt, Zn, Ag, Mg)^[15] are able to create nanoporous structures with higher edge/corner sites; d) the lattice strain of catalyst induced by the volume expansion/compression of the battery materials as underneath supports, resulting in changed electronic properties.^[16] Therefore, this

Dr. Z. Lu, Dr. G. Chen, Prof. Y. Cui
Department of Material Science and Engineering
Stanford University
Stanford, CA 94305, USA
E-mail: yicui@stanford.edu

Dr. K. Jiang, Dr. H. Wang
Rowland Institute
Harvard University
Cambridge, MA 02142, USA
E-mail: hwang@rowland.harvard.edu

Dr. H. Wang
Department of Chemical and Biomolecular Engineering
Rice University
Houston, TX 77005, USA

Prof. Y. Cui
Stanford Institute for Materials and Energy Science
SLAC National Accelerator Laboratory
Menlo Park, CA 94025, USA

 The ORCID identification number(s) for the author(s) of this article can be found under <https://doi.org/10.1002/adma.201800978>.

DOI: 10.1002/adma.201800978

LiET methodology almost covers a large portion of important electrocatalysts in this field, and thus can be considered as a new direction for discovering low-cost and highly efficient electrocatalysts for broad and important catalytic reactions.

In this progress report, based on each aforementioned category, we introduce the unique advantages of the LiET method and present the recent developments in employing this method to tune electrocatalysts for improving the performances of specific electrochemical reactions. The electrochemical tuning details, structural and electrochemical characterizations are also included. Finally, we put forward several interesting future directions of this LiET method and its applications in electrocatalysis.

2. Demonstrations of Electrochemical Tuning Method with Different Mechanisms

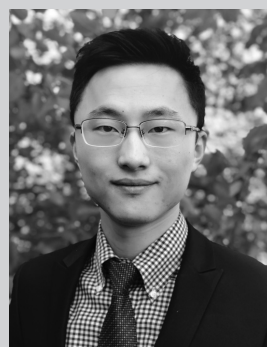
2.1. Intercalation/Deintercalation of Lithium Ions

The process of lithium-ion intercalation is able to tune the chemical potential of the target materials downward, accompanying with the oxidation state and local coordination configuration change of the catalytic site. Layered D materials (e.g., MoS₂ and WS₂), with strong covalent bonding within molecular layers and weak van der Waals interaction between layers, are an interesting family of materials for lithium intercalation.^[17] It is reported that, after chemical intercalation of Li (using n-butyl lithium as the reagent) and exfoliation, MoS₂ and WS₂ can be tuned from commonly semiconducting 2H phase to metallic 1T phase (Figure 1a–c), along with a lower oxidation state of the metal center.^[18] Additionally, the HER activities of exfoliated MS₂ (M = Mo and W) are significantly improved, which are mainly attributed to the more desirable electronic structures of metal centers induced by chemical Li intercalation.^[18a,b,19] However, in this method, the degree of intercalated Li can hardly be controlled due to the fast intercalation rate, and thereby the relationship between electronic structure and performance evolution are rarely obtained.

Electrochemical lithium intercalation, where the lithium ions migrate from the lithium-containing side to the target material side along with the injection of electrons, is a continuously tuning process and thus offer a platform for investigating the structure-activity relationship detailly. Our group initially synthesized vertically aligned MoS₂ nanofilm^[20]; moreover, the electronic structure of MoS₂ can be continuously tuned, and the corresponding HER catalytic activity is continuously improved upon electrochemical Li intercalation.^[10a,b] Figure 1d illustrates the battery configuration for Li electrochemical intercalation into the edge-terminated MoS₂ nanofilms. The amount of intercalated Li can be precisely controlled by the battery testing system. Therefore, the chemical potential of MoS₂ is continuously tuned. The discharge curve in Figure 1e provides useful information on the tuning of electronic structure of MoS₂ during Li intercalation. The intercalated Li donates electrons to the MoS₂ layers accompanied with the reduced oxidation state of Mo. The well-defined plateau between 1.2 and 1.1 V versus Li⁺/Li suggests a phase transition from 2H to 1T. The HER activities of MoS₂ nanofilms stopped at different intercalation voltages show the



Zhiyi Lu gained his B.E. degree from the College of Science and Ph.D. degree from the Department of Chemical Engineering, Beijing University of Chemical Technology in 2010 and 2015, respectively. Currently, he is a postdoc fellow under the supervision of Prof. Yi Cui in the Department of Materials Science and Engineering, Stanford University. His research interests focus on controlled synthesis of inorganic materials and investigating their broad electrocatalytic performance.

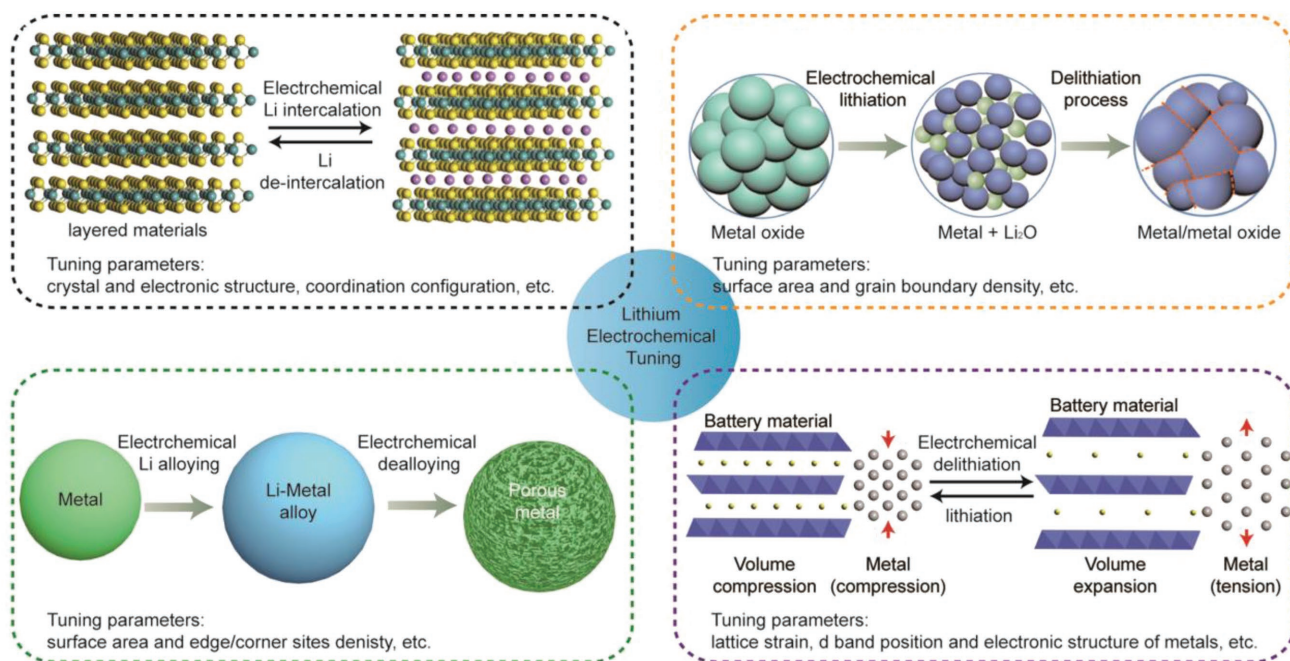


Haotian Wang is currently a Rowland Fellow and principle investigator at Harvard. In 2018, he joined Rice University, where in 2019 he will become the William Marsh Rice Trustee Chair Assistant Professor in the Department of Chemical and Biomolecular Engineering. He obtained his Ph.D. degree in applied physics from Stanford University in 2016 and B.S. degree in physics at USTC in 2011. His research group has been focused on developing novel nanomaterials for energy and environmental applications including energy storage, chemical/fuel generation, and water treatment.



Yi Cui is a professor in the Department of Materials Science and Engineering at Stanford University. He also holds a joint appointment in Photon Science Faculty, SLAC National Accelerator Laboratory. He obtained his B.S. degree in chemistry from the University of Science and Technology of China in 1998 and his Ph.D. degree in chemistry from Harvard University in 2002. He received the prestigious Miller Postdoctoral Fellowship to work at the University of California, Berkeley. In 2005, he became an assistant professor at Stanford University and obtained tenure in 2010.

trend of the tuning effects (Figure 1f). Lower intercalation voltages with lower oxidation states of Mo result in better HER performances; moreover, the 1T phase MoS₂ has a higher HER activity than that of 2H phase. The Tafel slope of 1T phase MoS₂ is measured as 44 mV dec⁻¹, which is significantly improved from the pristine MoS₂ of ≈120 mV dec⁻¹, as shown in Figure 1g.



Scheme 1. Scheme of the tuning function for catalysts based on the different reaction mechanisms in LIBs.

As a reverse process to electrochemical Li intercalation, electrochemical Li de-intercalation is a process where an external electrical power source is applied to force the lithium ions move out from the materials originally containing lithium. In this process, the chemical potential of the lithium-containing material is continuously tuned upward, which may be desirable for oxidative reactions, such as OER.

Indeed, it is found that unintentionally tuning of the catalyst surface would always happen to reach a more stable surface under the strong oxidative environment (i.e., during electrochemical OER). For example, the oxidation state of Ni or Co active centers in the catalysts (e.g., Ni(OH)₂ and Co₃O₄) would be increased under OER condition.^[21] In another case, it is reported that transition metal dichalcogenides can be in situ oxidized in strong alkaline media via an electrochemical oxidation process.^[22] Therefore, we propose that through electrochemical Li deintercalation at an organic medium, the catalyst can be tuned to possess a more stable surface under oxidation condition, which cannot be reached by the unintentionally tuning in aqueous solution.

Lithium cobalt oxide (LiCoO₂, denoted as LCO) is a typical example for this concept because the lithium ions are readily to be extracted out by simply applying an external bias and this material contains active Co center for OER.^[23] Our group demonstrates that continuous charging process to a critical potential (e.g., 4.3 V vs Li⁺/Li) can convert the pristine hexagonal LCO into monoclinic Li_{0.5}CoO₂ (Figure 1h) in organic electrolyte. For subsequent use as OER catalysts in aqueous electrolyte, the delithiated LiCoO₂ (De-LiCoO₂, the LCO after electrochemical tuning process) shows a remarkable enhancement in terms of the onset overpotential (Figure 1i), while negligible improvements are observed on other delithiated samples which do not achieve the critical potential (≈3.9 V), as shown in Figure 1j.^[10c] Moreover, we also find that this enhancement

is facet-dependent and can be attributed to the increase of the number of Co⁴⁺ sites and its strong covalent coupling to oxygen 2p states.^[10f] Beyond LCO, the LiET process is also applicable for other layered lithium transition metal oxides lithium and transition metal phosphates for improving their catalytic activities over water oxidation.^[10d]

2.2. Lithium Induced Conversion Reaction

Since the publication of the pioneering work by Kanan's group^[24] reporting that oxide-derived Cu shows an extraordinary activity for electrocatalytic CO reduction, this oxide-derived (OD) metal catalysts by electrochemical methods have attracted particular interest and the grain boundaries (GBs) existed in the OD-metals (Figure 2a,b) are identified that are active for electrocatalysis.^[25] In addition, the high activity of GBs for electrocatalysis can also be observed in metal oxides.^[26] Generally, the GBs are rich in lattice defects, dislocations, distortions, or local strains, thus offering unique electronic structures of metal centers. However, the different material properties of different metal oxides as well as the electrochemical reduction conditions trigger the different GB densities in OD metals. For example, ZnO and Bi₂O₃ would be slowly reduced at negative potentials because of their relatively low electrical conductivities. The small oxide nanoparticles (NPs) could get merged together into bulk crystalline during the reduction process, thus decreasing the GB densities.^[27] Therefore, developing a desirable process that can maintain or even increase the density of GBs is intriguing for boosting the electrocatalytic activities of metal/metal oxide catalysts.

Inspired by previous works in transition metal oxide (TMO) lithium-ion batteries, we assume that dramatic structural change can be found in the TMO materials after several lithiation and

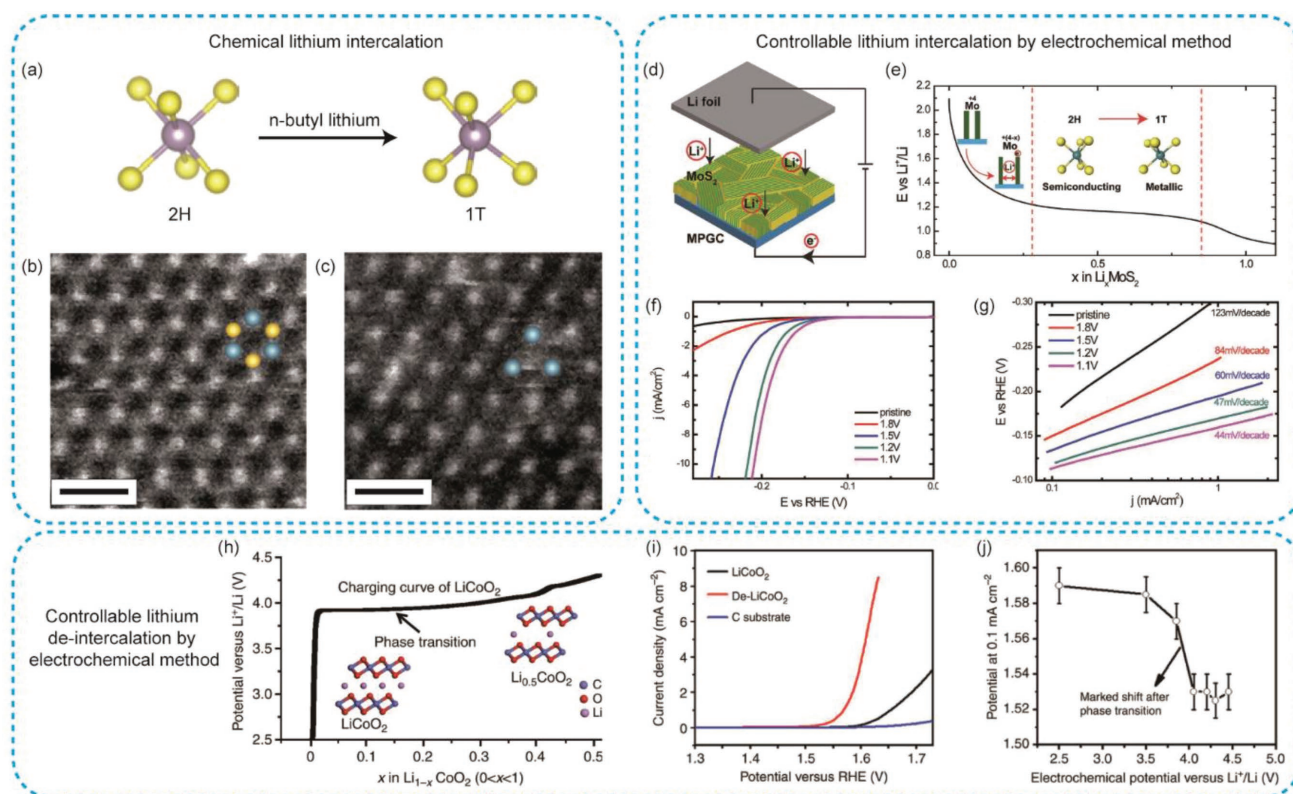


Figure 1. a) Schematic illustration of the phase transformation process of MoS₂ (from 2H to 1T) by chemical lithium intercalation. Atom color code: purple, Mo; yellow, S. Reproduced with permission.^[18a] Copyright 2013, Nature Publishing Group. b,c) Dark-field scanning transmission electron microscopy image of single-layer MoS₂ with different configurations. Scale bar: 0.5 nm. b,c) Reproduced with permission.^[18c] Copyright 2012, The American Chemical Society. d) Schematic of the battery testing system: the cathode is an MoS₂ nanofilm with molecular layers perpendicular to the substrate, where the green and yellow colors represent the edge sites and the terrace sites, respectively, and the anode is the Li foil. e) Galvanostatic discharge curve representing the lithiation process. f,g) Polarization curves and the corresponding Tafel plots of the pristine and lithiated MoS₂ nanofilms at different voltages. d–g) Reproduced with permission.^[10a] Copyright 2013, National Academy of Sciences. h) A typical charging curve of LiCoO₂: the crystal structure of the material and the electronic structure of the Co atom are both changed after phase transition, which occurred at the potential of 3.9–4 V versus Li⁺/Li. i) Polarization curves of LiCoO₂ and De-LiCoO₂. j) Plots of the electrochemical tuning potentials versus required OER potentials of LiCoO₂ at 0.1 mA cm⁻². h–j) Reproduced with permission.^[10c] Copyright 2014, Nature Publishing Group.

delithiation processes. Detailly, the Li conversion reaction ($\text{MO} + 2\text{Li}^+ + 2\text{e}^- \rightleftharpoons \text{M} + \text{Li}_2\text{O}$) takes place by breaking the M–O bonds and forming M–M and Li–O bonds in the lithiation process. The size of the transition metal materials would be greatly shrunk because of the removal of oxygen and new M–M bond formation. Once lithium is induced to react with TMO and then took out (i.e., delithiation process) whether electrochemically or chemically, the initial TMO materials would be transformed into much smaller interconnected metal/metal oxide NPs with few nanometers in diameter, as schemed in Figure 2c.^[10e] This structure change is confirmed by TEM characterizations where a single crystalline CoO NP can be successfully converted into ultra-small interconnected NPs after two cycles of Li charging and discharging process (Figure 2d,e). Moreover, the morphological transformation gives rise to increased surface area as well as GB densities of TMOs tremendously, which presents an ideal structure for highly active and stable electrochemical water splitting over 200 hours (the catalyst is 2-cycle NiFeO_x/CFP, as shown in Figure 2f). In another case, we have demonstrated that ZnO derived Zn catalyst by the LiET method (LiET-Zn) possesses much more abundant GBs (Figure 2g–i),

resulting in improved CO₂RR selectivity to CO compared with OD-Zn by traditional reduction method (Figure 2j).^[28]

2.3. Lattice Strain Tuning via LiET of Battery Electrode Materials

Previous reports have revealed that the lattice strain tuning is a powerful strategy to control the electronic structures of catalysts and thus tune their performances.^[29] Lattice strain, either compressive or tensile, can alter the surface electronic structure by modifying the distances between surface atoms and in turn catalytic activity. For platinum (Pt), previous studies have suggested that the 5d-band center of Pt can be shifted by ≈0.1 eV with only 1% lattice strain, which can appreciably strengthen or weaken bonding of ORR intermediates to the surface, as shown in Figure 3a,b.^[30] Due to the lattice-mismatch between Pt and other metals, the common strategy to achieve the lattice strain is to directly synthesize core–shell structures^[31] or selectively remove atoms from an alloy,^[32] as schemed in Figure 3c. However, because of the larger lattice of Pt as compared with that of most metal cores, this method is typically restricted to

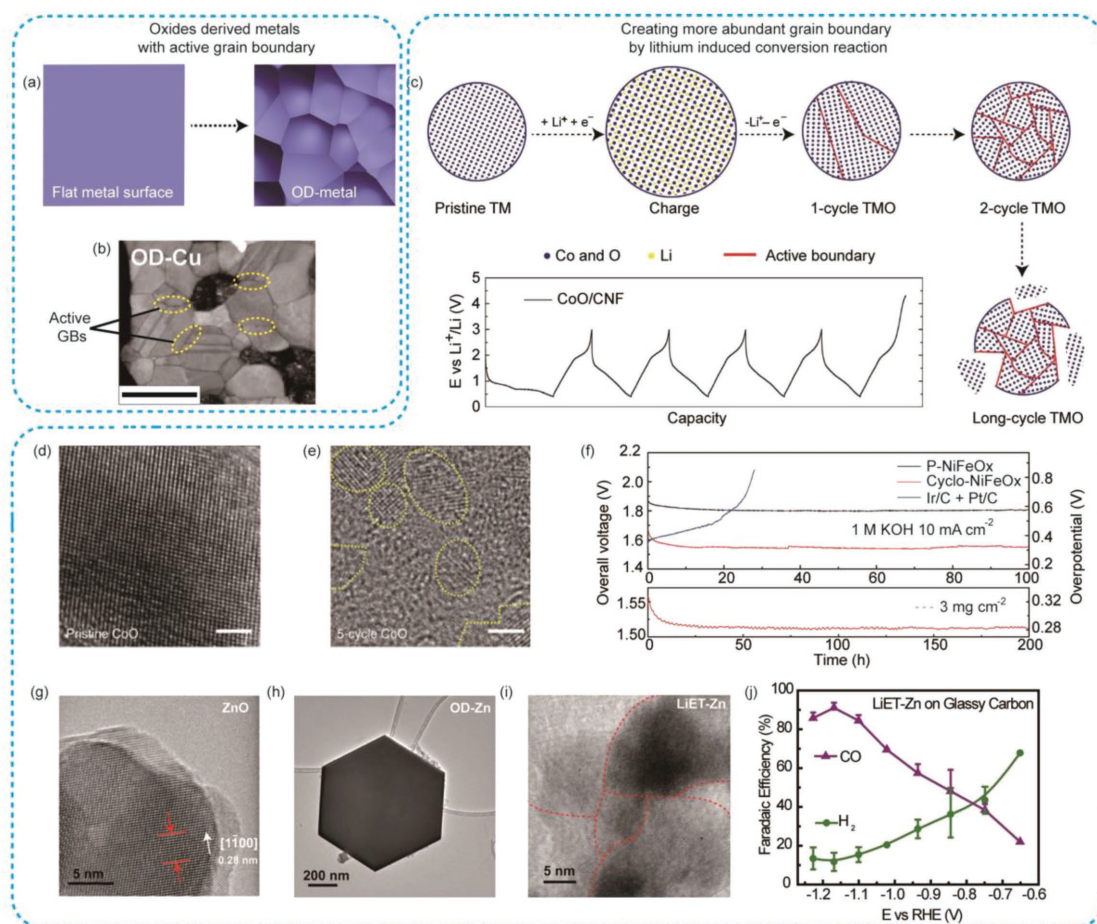


Figure 2. a,b) Scheme and SEM image of OD-metal surface with active GBs. b) Reproduced with permission.^[25c] Copyright 2015, The American Chemical Society. c) Transition metal oxide (TMO) particles gradually change from single crystalline to ultrasmall interconnected crystalline nanoparticles by battery cycling and the representative galvanostatic cycling profile of CoO/CNF composites. d,e) TEM images of a single crystalline CoO particle and ultrasmall interconnected CoO NPs after two cycles of Li charging and discharging process. f) Long-term overall water splitting stability of the 2-cycle NiFeO_x/CFP bifunctional catalyst with different mass-loadings. c–f) Reproduced with permission.^[10e] Copyright 2015, Nature Publishing Group. g–j) TEM images of pristine ZnO NPs, OD-Zn by traditional in situ electrochemical reduction under CO₂RR conditions, and LiET Zn with interconnected Zn NPs and enriched GBs by Li⁺ charging/discharging cycles. j) Faradaic efficiency of LiET-Zn for CO₂RR. g–j) Reproduced with permission.^[28] Copyright 2017, The American Chemical Society.

compressive strain,^[29a,33] except for metal cores with larger lattice such as Pb.^[34] Additionally, both electronic charge transfer between the different metal atoms (ligand effects) and changes in the surface stability—and thus surface area—are present, making it difficult to identify and control the effects of strain alone.^[29a] Another strategy is to deposit catalysts onto flat substrates that undergoes physical transformations with external forces or temperatures.^[35] Although those flat and tunable substrates are of great importance for fundamental analysis, only a few of them have been demonstrated effective in electrocatalysis.^[35a]

The LIBs research have shown that the battery electrode materials usually undergo significant volume changes during charging or discharging processes. This is a major reason why battery finally fails after many cycles due to the electrode damage under repeated volume expansion and compression. However, this disadvantage in battery research becomes a great opportunity in catalysis to introduce lattice strain. When lithium ions are electrochemically intercalated into or extracted out of electrode

materials such as graphite, transition-metal dichalcogenides, silicon, or Li metal oxides, the volume and lattice spacing change from several percent to several fold.^[36] For example, the Si electrode can expand up to four times its original size when fully lithiated to Li_{4.4}Si,^[36a] and LCO undergoes ≈3% volume changes during charge and discharge.^[36b] This smaller value is still sufficient to generate strain that can alter catalysis.

Our group first proved the idea by tuning the lattice strain on Pt catalysts with LCO as the tunable support. In LCO, lithium ions are sandwiched by Co-O octahedra slabs, and during charging, half of the Li⁺ are extracted to form Li_{0.5}CoO₂ (L_{0.5}CO). The Co-O slabs with negative charge experience stronger electrostatic repulsions from each other, which increases the layer spacing. When Li⁺ intercalates back during discharge, the lattice returns to its original spacing.^[37] To introduce lattice strain on Pt catalysts, small Pt NPs (≈5 nm) were deposited onto the surface of LCO or L_{0.5}CO particle supports (≈500 nm) using atomic layer deposition method. By controlling the charging or discharging states of the substrate (Figure 3d), we directly observed ≈5%

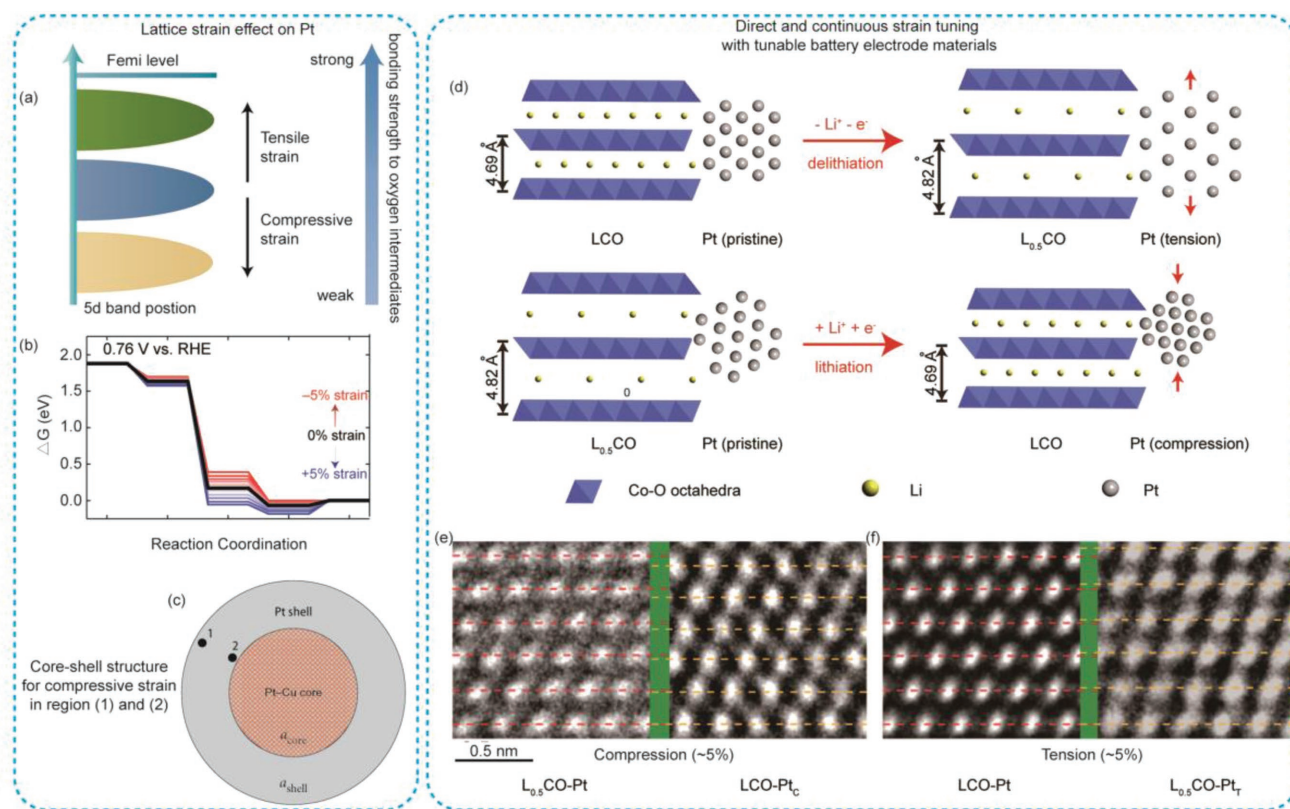


Figure 3. a) Scheme of the lattice strain effect on the Pt catalyst. The 5d band position and the bonding strength to oxygen intermediates would be tuned by the lattice strain. Note that our schematic only represents the position of d-band center and does not present an accurate description of the DOS in Pt d-band. b) The free-energy diagram for ORR at 0.76 V versus RHE, where all steps for the -5% strained Pt(111) are exergonic. b) Reproduced with permission.^[16] Copyright 2016, AAAS. c) Scheme of compressive strain of Pt by synthesizing a core-shell structure. Reproduced with permission.^[29] Copyright 2010, Nature Publishing Group. d) Schematic of the lattice constant change of LCO substrates and how the lattice strains are induced to Pt NPs. e, f) High-resolution TEM images of pristine and strained Pt NPs with (111) lattice compression and tension. d–f) Reproduced with permission.^[16] Copyright 2016, AAAS.

compressive and tensile strain on Pt (111) facets using transmission electron aberration-corrected microscopy (TEAM) in individual particles (Figure 3e,f).^[16] To have an intuitive understanding of how much the lattice strain is, we aligned the (111) atomic layers. After five layers of accumulation in spacing differences, the top layer of compressed Pt locates to a much lower

position than that of the pristine Pt, and that of the expanded Pt locates to a much higher position, offering direct evidences of the lattice strain. Accordingly, the ORR catalytic activities of Pt NPs in alkaline solution can also be tuned over a wide range, achieving nearly 90% improvement or more than 40% decrease in activity under compressive and tensile strain, respectively.

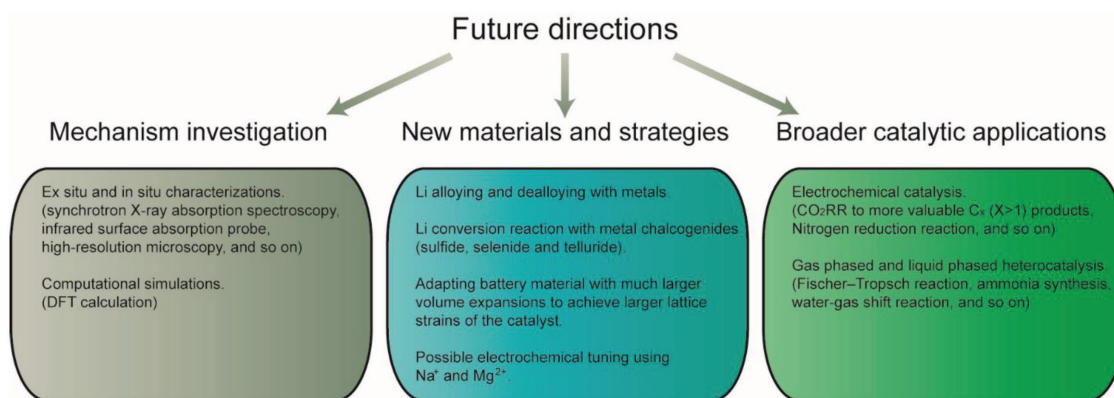


Figure 4. Proposed future directions of LiET method for catalysis.

3. Future Directions

The LIB technology has been maturely developed in the past few decades, and various materials whose electronic structures can be changed by reacting with lithium have been screened with their potentials for LIBs. In addition, the LIB technology offers a large thermodynamic potential range for continuous tuning the electronic structures. Therefore, the diversity and generality have made this LiET methodology as a powerful approach to explore advanced catalysts. Although several examples on this topic have been demonstrated by our group, many important works are still remaining unresolved and need to be further investigated in the future, as demonstrated in **Figure 4**.

First, it is interesting and necessary to understand how the catalysts after LiET affect the catalysis. As this process is related to the oxidation state, crystal structure and electronic structure of the catalyst, the investigation may require detailed ex situ and in situ characterizations, such as synchrotron X-ray absorption spectroscopy, infrared surface absorption probe, high-resolution microscopy, and so on, as well as simulation supports.

Second, besides these several successful examples, many other materials can also be tuned by this LiET method. For example, the metals with the ability to alloy with Li can undergo an alloying-dealloying process to reach a nanoporous structure with higher edge/corner sites density. We can also apply the Li induced conversion reaction strategy to transition metal sulfide, selenide and telluride.^[38] As the anion atoms (S, Se, and Te) are much bigger than oxygen, much more vacant space can be created during reduction and thus more GBs may be created when Li is extracted whether chemically or electrochemically. Another proposed direction is to adapt battery material that would undergo a much larger volume expansion to achieve a larger lattice strain of the catalyst.

Inspired by this LiET method, the recent development of other types of batteries (e.g., sodium^[39] and magnesium ion batteries^[40]) allows the Na and Mg electrochemical tuning becoming accessible. As the cations are much bigger than Li, the tuning effects on the catalysts would be different. Thus, electrochemical tuning the catalysts by other cations is an interesting direction to pursue.

Lastly, given the wide variety of tunable battery electrode materials in existence, this LiET methodology can be a highly general approach to design new catalytic materials not only for the aforementioned electrochemical reactions, but also for other electrocatalysis (e.g., CO₂RR to more valuable products^[41] and nitrogen reduction reaction^[42]) and thermal catalysis (e.g., Fischer–Tropsch reaction,^[43] methane activation^[44] and water-gas shift reaction^[45]) in the future.

Acknowledgements

The authors acknowledge support from SUNCAT seed funding in SLAC. K.J. and H.W. also acknowledge support from the Rowland Fellows Program at the Rowland Institute of Harvard University.

Conflict of Interest

The authors declare no conflict of interest.

Keywords

electrocatalysis, electrochemical tuning, transition metal oxides, 2D materials

Received: February 10, 2018

Revised: May 31, 2018

Published online:

- [1] A. Lasia, *Handbook of Fuel Cells*, John Wiley & Sons, Ltd., Chichester, UK **2010**.
- [2] M. Risch, J. Suntivich, Y. Shao-Horn, in *Encyclopedia of Applied Electrochemistry* (Eds: G. Kreysa, K.-i. Ota, R. F. Savinell), Springer Science+Business Media, New York **2014**, p. 1475.
- [3] M. Lefèvre, E. Proietti, F. Jaouen, J.-P. Dodelet, *Science* **2009**, *324*, 71.
- [4] D. Strmcnik, M. Uchimura, C. Wang, R. Subbaraman, N. Danilovic, D. Van Der Vliet, A. P. Paulikas, V. R. Stamenkovic, N. M. Markovic, *Nat. Chem.* **2013**, *5*, 300.
- [5] a) M. Liu, Y. Pang, B. Zhang, P. De Luna, O. Voznyy, J. Xu, X. Zheng, C. T. Dinh, F. Fan, C. Cao, *Nature* **2016**, *537*, 382; b) B. A. Rosen, A. Salehi-Khojin, M. R. Thorson, W. Zhu, D. T. Whipple, P. J. Kenis, R. I. Masel, *Science* **2011**, *334*, 643; c) K. Jiang, S. Siahrostami, A. J. Akey, Y. Li, Z. Lu, J. Lattimer, Y. Hu, C. Stokes, M. Gangishetty, G. Chen, Y. Zhou, W. Hill, W.-B. Cai, D. Bell, K. Chan, J. K. Nørskov, Y. Cui, H. Wang, *Chem* **2017**, *3*, 950; d) K. Jiang, R. B. Sandberg, A. J. Akey, X. Liu, D. C. Bell, J. K. Nørskov, K. Chan, H. Wang, *Nat. Catal.* **2018**, *1*, 111; e) K. Jiang, S. Siahrostami, T. Zheng, Y. Hu, S. Hwang, E. Stavitski, Y. Peng, J. J. Dynes, M. Gangishetty, D. Su, *Energy Environ. Sci.* **2018**, *11*, 893.
- [6] a) C. G. Morales-Guio, L.-A. Stern, X. Hu, *Chem. Soc. Rev.* **2014**, *43*, 5257; b) Y. Li, H. Dai, *Chem. Soc. Rev.* **2014**, *43*, 5257; c) M. G. Walter, E. L. Warren, J. R. McKone, S. W. Boettcher, Q. Mi, E. A. Santoro, N. S. Lewis, *Chem. Rev.* **2010**, *110*, 6446; d) J. S. Lee, S. Tai Kim, R. Cao, N. S. Choi, M. Liu, K. T. Lee, J. Cho, *Adv. Energy Mater.* **2011**, *1*, 34; e) R. O'hayre, S.-W. Cha, F. B. Prinz, W. Colella, *Fuel Cell Fundamentals*, John Wiley & Sons, Hoboken, NJ, USA **2016**.
- [7] a) Y. Liang, Y. Li, H. Wang, J. Zhou, J. Wang, T. Regier, H. Dai, *Nat. Mater.* **2011**, *10*, 780; b) K. Gong, F. Du, Z. Xia, M. Durstock, L. Dai, *Science* **2009**, *323*, 760; c) V. R. Stamenkovic, B. Fowler, B. S. Mun, G. Wang, P. N. Ross, C. A. Lucas, N. M. Marković, *Science* **2007**, *315*, 493; d) G. Wu, K. L. More, C. M. Johnston, P. Zelenay, *Science* **2011**, *332*, 443; e) V. Stamenkovic, B. S. Mun, K. J. Mayrhofer, P. N. Ross, N. M. Markovic, J. Rossmeisl, J. Greeley, J. K. Nørskov, *Angew. Chem., Int. Ed.* **2006**, *118*, 2963; f) A. Vojvodic, J. K. Nørskov, *Science* **2011**, *334*, 1355; g) C. C. McCrory, S. Jung, J. C. Peters, T. F. Jaramillo, *J. Am. Chem. Soc.* **2013**, *135*, 16977; h) J. Suntivich, K. J. May, H. A. Gasteiger, J. B. Goodenough, Y. Shao-Horn, *Science* **2011**, *334*, 1383; i) M. W. Kanan, D. G. Nocera, *Science* **2008**, *321*, 1072; j) B. Zhang, X. Zheng, O. Voznyy, R. Comin, M. Bajdich, M. García-Melchor, L. Han, J. Xu, M. Liu, L. Zheng, *Science* **2016**, *352*, 333; k) T. F. Jaramillo, K. P. Jørgensen, J. Bonde, J. H. Nielsen, S. Horch, I. Chorkendorff, *Science* **2007**, *317*, 100; l) B. Hinnemann, P. G. Moses, J. Bonde, K. P. Jørgensen, J. H. Nielsen, S. Horch, I. Chorkendorff, J. K. Nørskov, *J. Am. Chem. Soc.* **2005**, *127*, 5308.
- [8] J. Greeley, T. F. Jaramillo, J. Bonde, I. Chorkendorff, J. K. Nørskov, *Nat. Mater.* **2006**, *5*, 909.
- [9] a) H. Vrubel, D. Merki, X. Hu, *Energy Environ. Sci.* **2012**, *5*, 6136; b) J. Kibsgaard, Z. Chen, B. N. Reinecke, T. F. Jaramillo, *Nat. Mater.* **2012**, *11*, 963; c) Y. Li, H. Wang, L. Xie, Y. Liang, G. Hong, H. Dai, *J. Am. Chem. Soc.* **2011**, *133*, 7296; d) Z. Lu, W. Zhu, X. Yu,

- H. Zhang, Y. Li, X. Sun, X. Wang, H. Wang, J. Wang, J. Luo, X. Lei, L. Jiang, *Adv. Mater.* **2014**, 26, 2683.
- [10] a) H. Wang, Z. Lu, S. Xu, D. Kong, J. J. Cha, G. Zheng, P.-C. Hsu, K. Yan, D. Bradshaw, F. B. Prinz, Y. Cui, *Proc. Natl. Acad. Sci. USA* **2013**, 110, 19701; b) H. Wang, Z. Lu, D. Kong, J. Sun, T. M. Hymel, Y. Cui, *ACS Nano* **2014**, 8, 4940; c) Z. Lu, H. Wang, D. Kong, K. Yan, P.-C. Hsu, G. Zheng, H. Yao, Z. Liang, X. Sun, Y. Cui, *Nat. Commun.* **2014**, 5, 4345; d) Y. Liu, H. Wang, D. Lin, C. Liu, P.-C. Hsu, W. Liu, W. Chen, Y. Cui, *Energy Environ. Sci.* **2015**, 8, 1719; e) H. Wang, H.-W. Lee, Y. Deng, Z. Lu, P.-C. Hsu, Y. Liu, D. Lin, Y. Cui, *Nat. Commun.* **2015**, 6, 7261; f) Z. Lu, G. Chen, Y. Li, H. Wang, J. Xie, L. Liao, C. Liu, Y. Liu, T. Wu, Y. Li, *J. Am. Chem. Soc.* **2017**, 139, 6270.
- [11] a) V. Etacheri, R. Marom, R. Elazari, G. Salitra, D. Aurbach, *Energy Environ. Sci.* **2011**, 4, 3243; b) J. B. Goodenough, K.-S. Park, *J. Am. Chem. Soc.* **2013**, 135, 1167; c) J. B. Goodenough, Y. Kim, *Chem. Mater.* **2009**, 22, 587; d) Y. Sun, N. Liu, Y. Cui, *Nat. Energy* **2016**, 1, 16071.
- [12] M. Chhowalla, H. S. Shin, G. Eda, L.-J. Li, K. P. Loh, H. Zhang, *Nat. Chem.* **2013**, 5, 263.
- [13] K. Mizushima, P. Jones, P. Wiseman, J. B. Goodenough, *Mater. Res. Bull.* **1980**, 15, 783.
- [14] P. Poizot, S. Laruelle, S. Grugeon, L. Dupont, J. Tarascon, *Nature* **2000**, 407, 496.
- [15] M. T. McDowell, S. W. Lee, W. D. Nix, Y. Cui, *Adv. Mater.* **2013**, 25, 4966.
- [16] H. Wang, S. Xu, C. Tsai, Y. Li, C. Liu, J. Zhao, Y. Liu, H. Yuan, F. Abild-Pedersen, F. B. Prinz, J. K. Nørskov, Y. Cui, *Science* **2016**, 354, 1031.
- [17] a) J. Wilson, A. Yoffe, *Adv. Phys.* **1969**, 18, 193; b) M. Py, R. Haering, *Can. J. Phys.* **1983**, 61, 76; c) M. Dresselhaus, *MRS Bull.* **1987**, 12, 24.
- [18] a) D. Voiry, H. Yamaguchi, J. Li, R. Silva, D. C. Alves, T. Fujita, M. Chen, T. Asefa, V. B. Shenoy, G. Eda, *Nat. Mater.* **2013**, 12, 850; b) M. A. Lukowski, A. S. Daniel, F. Meng, A. Forticaux, L. Li, S. Jin, *J. Am. Chem. Soc.* **2013**, 135, 10274; c) G. Eda, T. Fujita, H. Yamaguchi, D. Voiry, M. Chen, M. Chhowalla, *ACS Nano* **2012**, 6, 7311; d) G. Eda, H. Yamaguchi, D. Voiry, T. Fujita, M. Chen, M. Chhowalla, *Nano Lett.* **2011**, 11, 5111.
- [19] a) D. Voiry, M. Salehi, R. Silva, T. Fujita, M. Chen, T. Asefa, V. B. Shenoy, G. Eda, M. Chhowalla, *Nano Lett.* **2013**, 13, 6222; b) M. A. Lukowski, A. S. Daniel, C. R. English, F. Meng, A. Forticaux, R. J. Hamers, S. Jin, *Energy Environ. Sci.* **2014**, 7, 2608.
- [20] a) D. Kong, H. Wang, J. J. Cha, M. Pasta, K. J. Koski, J. Yao, Y. Cui, *Nano Lett.* **2013**, 13, 1341; b) H. Wang, D. Kong, P. Johannes, J. J. Cha, G. Zheng, K. Yan, N. Liu, Y. Cui, *Nano Lett.* **2013**, 13, 3426.
- [21] a) M. W. Louie, A. T. Bell, *J. Am. Chem. Soc.* **2013**, 135, 12329; b) Z. Lu, W. Xu, W. Zhu, Q. Yang, X. Lei, J. Liu, Y. Li, X. Sun, X. Duan, *Chem. Commun.* **2014**, 50, 6479; c) B. S. Yeo, A. T. Bell, *J. Am. Chem. Soc.* **2011**, 133, 5587.
- [22] a) W. Chen, Y. Liu, Y. Li, J. Sun, Y. Qiu, C. Liu, G. Zhou, Y. Cui, *Nano Lett.* **2016**, 16, 7588; b) W. Chen, H. Wang, Y. Li, Y. Liu, J. Sun, S. Lee, J.-S. Lee, Y. Cui, *ACS Cent. Sci.* **2015**, 1, 244.
- [23] a) S. W. Lee, C. Carlton, M. Risch, Y. Surendranath, S. Chen, S. Furutsuki, A. Yamada, D. G. Nocera, Y. Shao-Horn, *J. Am. Chem. Soc.* **2012**, 134, 16959; b) T. Maiyalagan, K. A. Jarvis, S. Therese, P. J. Ferreira, A. Manthiram, *Nat. Commun.* **2014**, 5, 3949.
- [24] C. W. Li, J. Ciston, M. W. Kanan, *Nature* **2014**, 508, 504.
- [25] a) Y. Chen, C. W. Li, M. W. Kanan, *J. Am. Chem. Soc.* **2012**, 134, 19969; b) X. Feng, K. Jiang, S. Fan, M. W. Kanan, *ACS Cent. Sci.* **2016**, 2, 169; c) A. Verdaguier-Casadevall, C. W. Li, T. P. Johansson, S. B. Scott, J. T. McKeown, M. Kumar, I. E. Stephens, M. W. Kanan, I. Chorkendorff, *J. Am. Chem. Soc.* **2015**, 137, 9808.
- [26] Z. Zhang, J. Liu, J. Gu, L. Su, L. Cheng, *Energy Environ. Sci.* **2014**, 7, 2535.
- [27] K. Kamada, N. Enomoto, J. Hojo, *J. Ceram. Soc. Jpn.* **2009**, 117, 926.
- [28] K. Jiang, H. Wang, W.-B. Cai, H. Wang, *ACS Nano* **2017**, 11, 6451.
- [29] a) P. Strasser, S. Koh, T. Anniyev, J. Greeley, K. More, C. Yu, Z. Liu, S. Kaya, D. Nordlund, H. Ogasawara, *Nat. Chem.* **2010**, 2, 454; b) H. Li, C. Tsai, A. L. Koh, L. Cai, A. W. Contryman, A. H. Fragapane, J. Zhao, H. S. Han, H. C. Manoharan, F. Abild-Pedersen, J. Nørskov, X. Zheng, *Nat. Mater.* **2016**, 15, 48; c) M. Mavrikakis, B. Hammer, J. K. Nørskov, *Phys. Rev. Lett.* **1998**, 81, 2819.
- [30] B. Hammer, J. K. Nørskov, *Adv. Catal.* **2000**, 45, 71.
- [31] a) J. Zhang, F. Lima, M. Shao, K. Sasaki, J. Wang, J. Hanson, R. Adzic, *J. Phys. Chem. B* **2005**, 109, 22701; b) D. Wang, H. L. Xin, R. Hovden, H. Wang, Y. Yu, D. A. Muller, F. J. DiSalvo, H. D. Abruña, *Nat. Mater.* **2013**, 12, 81; c) X. Wang, S.-I. Choi, L. T. Roling, M. Luo, C. Ma, L. Zhang, M. Chi, J. Liu, Z. Xie, J. A. Herron, *Nat. Commun.* **2015**, 6, 7594; d) L. Zhang, L. T. Roling, X. Wang, M. Vara, M. Chi, J. Liu, S.-I. Choi, J. Park, J. A. Herron, *Science* **2015**, 349, 412.
- [32] a) C. Chen, Y. Kang, Z. Huo, Z. Zhu, W. Huang, H. L. Xin, J. D. Snyder, D. Li, J. A. Herron, M. Mavrikakis, *Science* **2014**, 343, 1339; b) S. Koh, P. Strasser, *J. Am. Chem. Soc.* **2007**, 129, 12624; c) I. E. Stephens, A. S. Bondarenko, F. J. Perez-Alonso, F. Calle-Vallejo, L. Bech, T. P. Johansson, A. K. Jepsen, R. Frydendal, B. P. Knudsen, J. Rossmeisl, *J. Am. Chem. Soc.* **2011**, 133, 5485; d) L. Gan, R. Yu, J. Luo, Z. Cheng, J. Zhu, *J. Phys. Chem. Lett.* **2012**, 3, 934.
- [33] a) Q. Jia, W. Liang, M. K. Bates, P. Mani, W. Lee, S. Mukerjee, *ACS Nano* **2015**, 9, 387; b) X. Huang, Z. Zhao, L. Cao, Y. Chen, E. Zhu, Z. Lin, M. Li, A. Yan, A. Zettl, Y. M. Wang, X. Duan, T. Mueller, Y. Huang, *Science* **2015**, 348, 1230.
- [34] L. Bu, N. Zhang, S. Guo, X. Zhang, J. Li, J. Yao, T. Wu, G. Lu, J.-Y. Ma, D. Su, *Science* **2016**, 354, 1410.
- [35] a) M. Du, L. Cui, Y. Cao, A. J. Bard, *J. Am. Chem. Soc.* **2015**, 137, 7397; b) L. Yang, X. Cui, J. Zhang, K. Wang, M. Shen, S. Zeng, S. A. Dayeh, L. Feng, B. Xiang, *Sci. Rep.* **2014**, 4, 5649.
- [36] a) C. K. Chan, H. Peng, G. Liu, K. McIlwrath, X. F. Zhang, R. A. Huggins, Y. Cui, *Nat. Nanotech.* **2008**, 3, 31; b) T. Ohzuku, A. Ueda, *J. Electrochem. Soc.* **1994**, 141, 2972; c) G. Csányi, P. Littlewood, A. H. Nevidomskyy, C. J. Pickard, B. Simons, *Nat. Phys.* **2005**, 1, 42.
- [37] Y. Shao-Horn, L. Croguennec, C. Delmas, E. C. Nelson, M. A. O'Keefe, *Nat. Mater.* **2003**, 2, 464.
- [38] N. Nitta, F. Wu, J. T. Lee, G. Yushin, *Mater. Today* **2015**, 18, 252.
- [39] N. Yabuuchi, K. Kubota, M. Dahbi, S. Komaba, *Chem. Rev.* **2014**, 114, 11636.
- [40] R. C. Massé, E. Uchaker, G. Cao, *Sci. China Mater.* **2015**, 58, 715.
- [41] a) H. Wang, Y. Chen, X. Hou, C. Ma, T. Tan, *Green Chem.* **2016**, 18, 3250; b) A. Loiudice, P. Lobaccaro, E. A. Kamali, T. Thao, B. H. Huang, J. W. Ager, R. Buonsanti, *Angew. Chem., Int. Ed.* **2016**, 55, 5789.
- [42] M. M. Shi, D. Bao, B. R. Wulan, Y. H. Li, Y. F. Zhang, J. M. Yan, Q. Jiang, *Adv. Mater.* **2017**, 29, 1606550.
- [43] W. Chen, Z. Fan, X. Pan, X. Bao, *J. Am. Chem. Soc.* **2008**, 130, 9414.
- [44] P. Tang, Q. Zhu, Z. Wu, D. Ma, *Energy Environ. Sci.* **2014**, 7, 2580.
- [45] T. Bunluesin, R. Gorte, G. Graham, *Appl. Catal., B* **1998**, 15, 107.